Penerbit Akademia Baru

Journal of Advanced Research in Fluid Mechanics and Thermal Sciences
ISSN (online): 2289-7879 | Vol. 17, No. 1. Pages 1-17, 2016

Study of a Beam FGM under Loading Electrostatic

H. M. Berrabah[*,1,3], *N. Z. Sekrane*[1,2,a] *and B. E. Adda*[1,2,b]

[1]Département de Génie Civil, Centre Universitaire de Relizane, Relizane, Algérie.
[2]Département de Génie Civil, Université Djillali Liabes, Sidi Bel Abbes, Algérie.
[3]Laboratoire des Matériaux et Hydrologie, Sidi Bel Abbes, Algérie
[*]*b_hamza_2005@yahoo.fr,* [a] *n.sekrane@gmail.com,* [b]*addabed@yahoo.com*

Abstract-*Based on the theory of elasticity, some exact solutions of functionally gradient piezothermoelastic cantilevers under different coupled loadings are obtained. As an application, these solutions have been successfully used to identify the gradient piezoelectric parameter and the thermal material coefficients. Besides, some numerical results have been carried out for the cantilever under two different kinds of loadings. It is found that the tip deflection of the cantilever agrees very well with the experimental and theoretical findings provided by other investigations. The present study also shows that the linear change of thermal material parameters does not influence the distribution of the stress and induction of the cantilever. But it influences the components of strain and electric field strength as well as the displacement and electric potential of the cantilever. The analytical expressions have been derived for the through thickness stresses of a composite active FGM beam subjected to electrical excitation. The structure is comprised of a substrate, an electro-elastically graded layer and an active layer. Continuous gradation of the volume fraction in the FGM layer is modelled in the form of an mth power polynomial of the coordinate axis in thickness direction of the beam. A numerical scheme of discretizing the continuous FGM layer (in sub-layers) and treating the beam as a discretely graded structure has also been developed. Appropriate expressions for the solution have been derived for the case of continuous power law gradation (mth power) of the FGM layer. The discretized FGM layer scheme has been shown to yield results that practically match those predicted analytically by the closed-form model.*

Keywords – FGM, beam, electric potential, piezothermoelastic, elasticity, thermal material parameters.

1.0 INTRODUCTION

Since the discovery of the effect of piezoelectricity in 1880 by the Curie brothers, piezoelectric materials are widely applied in technology, such as research on piezoelectric ultrasonic motors the vibration control of various types of structures [1], actuator [2], etc. Applications in the art, piezoelectric materials are often designed in a monolayer or bilayer, are mechanically bonded by an adhesive layer presented a detailed discussion of deformation measurements in the piezoelectric ceramic (PZT) sensors and piezoelectric film (PVDF) compared with conventional strains. The main weaknesses of these devices are that sandwich the adhesive layer may crack at low temperatures and come off at high temperature, which will reduce the life and reliability of these piezoelectric devices. Sometimes the thermal load is far from being the main reason for the breakdown of these smart structures. Therefore, the effects of thermal loading have attracted particular attention in recent years. For example, [2] have discussed the properties and modeling of piezoelectric materials at moderately elevated temperatures. [2] presented a generalized formulation of finite elements piezo-thermo-elastic

a laminated beam with piezoelectric materials composed of sensor / actuator distributed. [2] studied the effects of temperature on piezoelectric sensors and substrate composite, and found that even moderate fluctuations of temperature about may change significantly the voltage reading from to a piezoelectric sensor. [3] have completed a numerical analysis of the thermomechanical behavior of the piezoelectric structures in finite deformations. To improve the durability of the piezoelectric structures, piezoelectric materials has gradient evaluated (FGPM) were developed and used to produce devices such as sensors and actuators [4]. When piezoelectric materials are designed with a gradual variation in the material considered in one or two dimensions, they can overcome the peeling and cracking of the adhesive layer and at the same time reduces the mechanical stress. Based on a simple analytical model, [5] studied a type of piezoelectric actuator multimorphe and predict the behavior of the actuators material has evaluated gradient (FGM). Using classical elasticity theory [6] gave some solutions not only for a beam console with properties varying gradually but a brief summary of the design and modeling for micro actuators console. [7] Compared the bending behavior and polymorphic bimorph actuators based on a finite element analysis. In general, several types of piezoelectric consoles are in the literature among them: there is a potential function for the surface forces, the piezoelectric parameter (g_{31}) changes linearly and finally the elastic parameter (S_{33}) and surface forces change simultaneously [8], the elastic analyzes are provided and fundamental solutions are obtained.

2.0 BASIC EQUATIONS FOR PIEZO-THERMO-ELASTIC MATERIALS IN PLANE STRAIN

The console beam used as a model for analysis of sensors and piezoelectric actuators [9], shown in Figure 1, is studied. The upper and lower surfaces of the beam are bonded in a continuous way to the electrodes. To describe the basic equations of the problem, a Cartesian coordinate system (x, z) is introduced into the analysis. represent respectively, the components of strain, stress, induction, and the electric field of the piezoelectric medium, the constitutive equations for a piezo-elastic material thermo-plane strain are expressed as follows [10]

$$\begin{cases} \varepsilon_x = S_{11}\sigma_x + S_{13}\sigma_z + g_{31}D_z - \mu_{11}\theta \\ \varepsilon_z = S_{13}\sigma_x + S_{33}\sigma_z + g_{33}D_z - \mu_{33}\theta \\ \gamma_{xz} = S_{44}\tau_{xz} + g_{15}D_x \end{cases} \quad (1)$$

$$\begin{cases} E_x = -g_{15}\tau_{xz} + \xi_{11}D_x \\ E_z = -g_{31}\sigma_x - g_{33}\sigma_z + \xi_{33}D_z - q_3\theta \end{cases} \quad (2)$$

where S_{ij}, g_{ij} and ξ_{ij} are respectively the flexibility coefficients, piezoelectric and dielectric impermeability; θ is the temperature; μ_{ii} and q_3 are respectively the thermal deformation and pyroelectric coefficients of the material. Without consideration of volume forces, the equilibrium equations can be written as

$$\begin{cases} \frac{\partial \sigma_x}{\partial x} + \frac{\partial \tau_{xz}}{\partial z} = 0 \\ \frac{\partial \tau_{xz}}{\partial x} + \frac{\partial \sigma_z}{\partial z} = 0 \end{cases} \quad (3)$$

Penerbit Akademia Baru

Journal of Advanced Research in Fluid Mechanics and Thermal Sciences
ISSN (online): 2289-7879 | Vol. 17, No. 1. Pages 1-17, 2016

$$\frac{\partial D_x}{\partial x}+\frac{\partial D_{xz}}{\partial z}=0 \tag{4}$$

$$\frac{\partial}{\partial x}(k_{11}\frac{\partial \theta}{\partial x})+\frac{\partial}{\partial z}(k_{33}\frac{\partial \theta}{\partial z})=0 \tag{5}$$

From equation (5), the first equation of the equation system is derived (3) with respect to x and the second with respect to z and makes the subtraction between the two equations, we will

$$\frac{\partial^2 \sigma_x}{\partial x^2}-\frac{\partial^2 \sigma_z}{\partial z^2}=0 \tag{6}$$

After simplification we obtained

$$\frac{\partial}{\partial x}(k_{11}\frac{\partial \theta}{\partial x})+\frac{\partial}{\partial z}(k_{33}\frac{\partial \theta}{\partial z})=0 \tag{7}$$

That is to say, after the elimination of all terms that depend on the system of equations (3) and (4), or

$$k_{11}=\frac{(-g_{33}S_{13}+g_{31}S_{33})q_3}{2S_{13}g_{31}g_{33}-g_{31}^2S_{33}+S_{13}^2\xi_{33}-g_{33}^2S_{11}-S_{11}S_{33}\xi_{33}}+\frac{(g_{33}g_{31}\mu_{33}-\mu_{11}S_{33}\xi_{33}+\mu_{33}S_{13}\xi_{33}-g_{33}^2\mu_{11})}{2S_{13}g_{31}g_{33}-g_{31}^2S_{33}+S_{13}^2\xi_{33}-g_{33}^2S_{11}-S_{11}S_{33}\xi_{33}}$$

$$k_{33}=-\frac{(-g_{33}S_{11}+g_{31}S_{13})q_3}{2S_{13}g_{31}g_{33}-g_{31}^2S_{33}+S_{13}^2\xi_{33}-g_{33}^2S_{11}-S_{11}S_{33}\xi_{33}}-\frac{(g_{31}^2\mu_{33}-\mu_{11}S_{13}\xi_{33}+\mu_{33}S_{11}\xi_{33}-g_{31}g_{33}\mu_{11})}{2S_{13}g_{31}g_{33}-g_{31}^2S_{33}+S_{13}^2\xi_{33}-g_{33}^2S_{11}-S_{11}S_{33}\xi_{33}} \tag{8}$$

where k_{ij} is the coefficient of thermal conductivity. Deformation of the components and the electric field are connected to the displacement (u,w) and the electric potential ϕ by the following equations

$$\begin{cases}\varepsilon_x=\dfrac{\partial u}{\partial x}\ ,\varepsilon_z=\dfrac{\partial w}{\partial z}\ ,\gamma_{xz}=\dfrac{\partial u}{\partial z}+\dfrac{\partial w}{\partial x}\\ E_x=-\dfrac{\partial \phi}{\partial x}\ ,\qquad E_z=-\dfrac{\partial \phi}{\partial z}\end{cases} \tag{9}$$

It is verified that the piezoelectric (g_{31}) parameter plays an important role in judging the behavior of piezoelectric materials and performance of piezoelectric products. Several studies [11] were made on the properties of piezoelectric materials with different values. In this chapter, we look at the exact solutions of piezo-thermo-elastic consoles beams. The gradient of the piezoelectric property (g_{31}) parameter is taken into consideration, while other hardware settings are assumed to be constants. Among them the property of the piezoelectric gradient parameter (g_{31}) is assumed as follows

$$g_{31}=r_1z+r_2 \tag{10}$$

Penerbit Akademia Baru

Journal of Advanced Research in Fluid Mechanics and Thermal Sciences
ISSN (online): 2289-7879 | Vol. 17, No. 1. Pages 1-17, 2016

where r_1 and r_2 are material constants. Equations (1) - (9) and the appropriate boundary conditions can be used to study the problem in question.

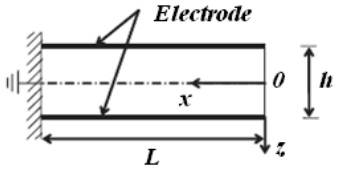

Figure 1: console piezoelectric

Substitution in equations (1) and (4) in equation (9), we have the following equations in terms of stress σ_x, σ_z, and induction D_x, D_z

$$\begin{cases} [S_{11}\dfrac{\partial}{\partial z^2}+(S_{13}+\dfrac{S_{44}}{2})\dfrac{\partial^2}{\partial x^2}]\sigma_x+[S_{33}\dfrac{\partial}{\partial x^2}+(S_{13}+\dfrac{S_{44}}{2})\dfrac{\partial^2}{\partial z^2}]\sigma_z+(r_1z+r_2)\dfrac{\partial^2 D_z}{\partial z^2} \\ +g_{33}\dfrac{\partial^2 D_z}{\partial x^2}+2r_1\dfrac{\partial D_z}{\partial z}-g_{15}\dfrac{\partial^2 D_x}{\partial x\partial z}-\mu_{11}\dfrac{\partial^2\theta}{\partial z^2}-\mu_{33}\dfrac{\partial^2\theta}{\partial x^2}=0 \\ (r_1z+r_2+g_{15})\dfrac{\partial\sigma_x}{\partial x}+g_{33}\dfrac{\partial\sigma_z}{\partial x}+\xi_{11}\dfrac{\partial D_x}{\partial z}-\xi_{33}\dfrac{\partial D_z}{\partial x}+q_3\dfrac{\partial\theta}{\partial x}=0 \end{cases} \quad (11)$$

For the equation (12), the equations are replaced (1), (2) in (9), uses the following equation compatibility

$$\frac{\partial^2\varepsilon_x}{\partial z^2}+\frac{\partial^2\varepsilon_z}{\partial x^2}=\frac{\partial^2\gamma_{xz}}{\partial x\partial z} \quad (12)$$

And from the system (3), the first equation of the system is derived (3) with respect to x and second with respect to z and made the addition, deduct the following Expression

$$\frac{\partial^2\tau_{xz}}{\partial x\partial z}=\frac{1}{2}(\frac{\partial^2\sigma_x}{\partial x^2}+\frac{\partial^2\sigma_z}{\partial z^2}) \quad (13)$$

For the second equation of the system (12), the equation is derived (15) with respect to (z) and will

$$E_x=-\frac{\partial\phi}{\partial x} \quad (14)$$

And Equation (16) to (x)

$$E_z=-\frac{\partial\phi}{\partial z} \quad (15)$$

And we do E_x - $E_z=0$ we obtain the second equation system (12). In effect, equation (12) is the compatibility equation to find the displacement and the electric potential when the strain and induction are already obtained.

Penerbit Akademia Baru

Journal of Advanced Research in Fluid Mechanics and Thermal Sciences
ISSN (online): 2289-7879 | Vol. 17, No. 1. Pages 1-17, 2016

3.0 THE EXACT SOLUTIONS OF A PIEZO-THERMO-ELASTIC CONSOLE UNDER COUPLED LOADS

For a piezoelectric console (Figure I), subjected to the charge-coupled (thermal and mechanical / electrical), the exact solutions can be determined based on the theory of elasticity, the temperature field can be easily obtained.

3.1 Temperature Field

Assume that the piezoelectric console is heated homogeneously on the upper surface, the temperature at the upper and lower surfaces of the beam is assumed to be constant and equal to θ_0 and 0 respectively. This means that we have the following thermal boundary conditions:

$$\theta(x,\frac{h}{2})=0 \quad , \quad \theta(x,-\frac{h}{2})=\theta_0 \tag{16}$$

In this case, equation (5) become

$$k_{33}\frac{\partial^2\theta}{\partial z^2}=0 \tag{17}$$

For the equation (16), it makes the solution of the differential equation (17). And the console of the temperature field can be easily obtained as follows

$$\theta=A+Bz \tag{18}$$

After using the boundary conditions (16) the values of A and B is expressed as follows

$$A=\theta_0/2 \ , \ B=-\theta_0/h \tag{19}$$

3.2 Mechanical and Electrical Fields

Using equation (18), the compatibility of equation (12) may be as follows

$$\begin{cases} [S_{11}\dfrac{\partial}{\partial z^2}+(S_{13}+\dfrac{S_{44}}{2})\dfrac{\partial^2}{\partial x^2}]\sigma_x+[S_{33}\dfrac{\partial}{\partial x^2}+(S_{13}+\dfrac{S_{44}}{2})\dfrac{\partial^2}{\partial z^2}]\sigma_z+(r_1z+r_2)\dfrac{\partial^2 D_z}{\partial z^2} \\ +g_{33}\dfrac{\partial^2 D_z}{\partial x^2}+2r_1\dfrac{\partial D_z}{\partial z}-g_{15}\dfrac{\partial^2 D_x}{\partial x\partial z}=0 \\ (r_1z+r_2+g_{15})\dfrac{\partial\sigma_x}{\partial x}+g_{33}\dfrac{\partial\sigma_z}{\partial x}+\xi_{11}\dfrac{\partial D_x}{\partial z}-\xi_{33}\dfrac{\partial D_z}{\partial x}=0 \end{cases} \tag{20}$$

To find the mechanical and electrical fields in the piezoelectric console, the Airy function is used. The constraint function (φ) and induction (ψ) function are introduced. The components of the strain and induction can be expressed as follows

$$\sigma_x=\frac{\partial^2\varphi}{\partial z^2} \ , \ \sigma_z=\frac{\partial^2\varphi}{\partial x^2} \ , \ \tau_{xz}=-\frac{\partial^2\varphi}{\partial x\partial z} \ , \ D_x=\frac{\partial\psi}{\partial z} \ , \ D_z=-\frac{\partial\psi}{\partial x} \tag{21}$$

Penerbit Akademia Baru
Journal of Advanced Research in Fluid Mechanics and Thermal Sciences
ISSN (online): 2289-7879 | Vol. 17, No. 1. Pages 1-17, 2016

To find the solutions, the two above types of coupled loads are taken separately.

Case I: console subject to thermal and electrical loads
In addition to thermal loading, the piezoelectric console is also subjected to an electrical load (Figure II), that is to say, there is a difference in electric potential between the upper and lower surface of the bracket

$$\phi(x,-\frac{h}{2})-\phi(x,\frac{h}{2})=V_0 \tag{22}$$

In this case, the stress and the induction function of function may be assumed as follows

$$\varphi=0 \quad , \quad \psi=bx \tag{23}$$

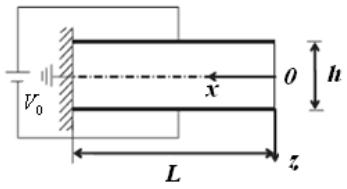

Figure 2: console subject has a loading thermal and fields electric

which b is an unknown constant to be determined. Substituting equation (20) in equation (19), the expressions of the stress and the induction can be obtained as

$$\sigma_x=\sigma_z=\tau_{xz}=D_x=0 \quad \text{et} \quad D_z=-b \tag{24}$$

It is obvious that the compatibility of equation (18) is automatically satisfied in this case. In addition, the stress and the induction satisfactory as all the following boundary conditions. Conditions to mechanical limits

$$\tau_{xz}=\sigma_z=0 \quad \text{a} \quad z=\pm h/2 \quad , \quad \tau_{xz}=\sigma_x=0 \quad \text{a} \quad x=0 \tag{25}$$

Boundary conditions electric

$$D_x=0 \qquad x=0,L \tag{26}$$

One using the equation (1), the distortion components and the electric field can be obtained as

$$\begin{cases}\varepsilon_x=-(r_1z+r_2)b-\mu_{11}(A+Bz)\\ \varepsilon_z=-g_{33}b-\mu_{33}(A+Bz)\\ \gamma_{xz}=0\end{cases} \tag{27}$$

$$\begin{cases}E_x=0\\ E_z=-\xi_{33}b-q_3(A+Bz)\end{cases} \tag{28}$$

Penerbit Akademia Baru
Journal of Advanced Research in Fluid Mechanics and Thermal Sciences
ISSN (online): 2289-7879 | Vol. 17, No. 1. Pages 1-17, 2016

To determine the displacement and the electric potential of the console, the following boundary conditions are considered

$$u(L,0)=0\,,\qquad w(L,0)=0\,,\quad \frac{\partial w}{\partial x}(L,0)=0\ ,\ \phi(L,0)=0 \tag{29}$$

By integrating the equation (9), and using the conditions motionnées limits above and equation (14), movement of the components and the electric potential and the unknown constant b can be determined as

$$\begin{cases} u=(r_1z+r_2)b(L-x)+\mu_{11}(A+Bz)(L-x) \\ w=-g_{33}b-\mu_{33}(Az+\dfrac{B}{2}z^2)+\dfrac{1}{2}(r_1b+B\mu_{11})(x^2-2xL+L^2) \end{cases} \tag{30}$$

$$\phi=\xi_{33}bz-q_3(Az+\frac{B}{2}z^2) \tag{31}$$

With

$$b=-\frac{q_3Ah+V_0}{\xi_{33}h} \tag{32}$$

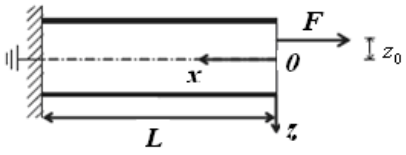

Figure 3: console subject has a loading thermal and load eccentric

The analysis and solutions above show that the coupled thermal and electrical loads do not lead to the stress components in the estimated gradient consoles. This finding shows that the proposal is correct. For distribution of the electric potential at any cross section of the beam, a quadratic approximate expression is found.

Case II: subject console has a thermal load and mechanical

For the piezoelectric console shown in Figure 3, and in addition thermal loading, an eccentric load F is applied to the free end. In this case, the stress and the induction function of function may be assumed the following expressions

$$\varphi=-az^3-cz^2\qquad,\quad \psi=0 \tag{33}$$

where a and c are unknown constants to be determined. In the following stress and the induction of components are obtained using Equation (19)

$$\sigma_x=-6az-2cz\qquad \sigma_z=\tau_{xz}=D_x=D_z=0 \tag{34}$$

It is obvious that the compatibility of equation (18) is satisfied. In addition, conditions for mechanical and electrical limits are also automatically checked as

Penerbit Akademia Baru
Journal of Advanced Research in Fluid Mechanics and Thermal Sciences
ISSN (online): 2289-7879 | Vol. 17, No. 1. Pages 1-17, 2016

$$\begin{cases} \sigma_z = \tau_{xz} = D_x = D_z = 0 & z = \pm h/2 \\ D_x = 0 & x = 0, L \end{cases} \tag{35}$$

To meet the requirements to the mechanical limitations to the free end of the console, the Saint-Venant principle is introduced

$$\tau_{xz} = 0 \quad , \quad \int_{-h/2}^{h/2} \sigma_x dz = F \quad , \quad \int_{-h/2}^{h/2} \sigma_x z dz = -Fz_0 \qquad x = 0 \tag{36}$$

Substituting equation (28) in equation (24), we obtain

$$a = \frac{2Fz_0}{h^3} \quad , \quad c = -\frac{F}{2h} \tag{37}$$

Using Equation (1), the components of strain and the electric field can be obtained as

$$\begin{cases} \varepsilon_x = -2S_{11}c - \mu_{11}A - (6S_{11}a - B\mu_{11})z \\ \varepsilon_z = -2S_{13}c - \mu_{33}A - (6S_{13}a - B\mu_{33})z \\ \gamma_{xz} = 0 \end{cases} \tag{38}$$

$$\begin{cases} E_x = 0 \\ E_z = 6ar_1 z^2 + (2cr_1 + 6ar_2 - q_3 B)z + 2cr_2 - q_3 A \end{cases}$$

(439)

In addition, the displacement and the electric potential can be obtained respectively as follows

$$\begin{cases} u = (2S_{11}c + \mu_{11}A)(L - x) + (6S_{11}a + B\mu_{11})(L - x)z \\ w = -\frac{1}{2}(6S_{13}a + \mu_{33}B)z^2 - (2S_{13}c + A\mu_{33})z + \frac{1}{2}(6S_{11}a + \mu_{11}B)(x^2 - 2xL + x^2) \end{cases} \tag{39}$$

$$\phi = -2ar_1 z^3 - \frac{1}{2}(2cr_1 + 6ar_2 - q_3 B)z^2 - (2cr_2 - q_3 A)z \tag{40}$$

It can be determined from this solution that all the stress components except σ_x are zero when the bracket is subjected to eccentric load and F a thermal load. A cubic expression for the electric potential distribution on any cross section of the console is also determined.

3.3 Parameter Identification

On the parameter identification plays a very important role in accurately describing the internal behavior of FGM type of material. For a graded material, it is very difficult to treat a homogeneous sample to measure the properties of a material point person using a method introduced by General [12]. Much attention has been given to identify a non-homogeneous materials. [13] determined the temperature field of a body contacting using a potential function approach including three potential displacement and two electrical potentials. [14] presented a method for computing inverse characterization of material properties of FGMs

using the surface displacement response of the plate. [15] measured the temperature dependency of the real and imaginary parts of coefficient S_{11}^{E} using the piezoelectric resonance method. [16] developed a simple technique for characterizing the elastic modulus of thin layers of any thickness. The method to identify hardware settings for functionally graded materials piezothermoelastic is studied by several authors.

3.4. Identification of the Piezoelectric Parameter (g_{31})

Based on the results above, the piezoelectric (g_{31}) parameter can be identified. To determine the unknown parameters (r_1 and r_2) in Equation (9), a bracket axially loaded by a concentrated force (F) at the free end, as shown in Figure (4) .Ignorant temperature the beam, the electrical potential of the beam can be obtained from equation (30) as

$$\phi = \frac{F}{2h} r_1 z^2 + \frac{F}{2h} r_2 z \tag{41}$$

Respectively ϕ_U and ϕ_L indicates the electrical potential on the upper and lower surfaces of the beam. Then the parameters (r_1 and r_2) can be found

$$r_1 = \frac{4(\phi_U - \phi_L)}{Fh} \quad , \quad r_2 = \frac{\phi_U - \phi_L}{F} \tag{42}$$

For parameters r_1 , r_2 ,, it was $\phi_L = \phi(h/2)$ and $\phi_U = \phi(-h/2)$ is to say

$$\phi_L = \frac{F}{2h} r_1 (\frac{h}{2})^2 + \frac{F}{2h} r_2 \frac{h}{2} \tag{43}$$

So

$$\phi_L = \frac{Fh}{8} r_1 + \frac{F}{2} r_2 \tag{44}$$

And

$$\phi_U = \frac{F}{2h} r_1 (-\frac{h}{2})^2 - \frac{F}{2h} r_2 \frac{h}{2} \tag{45}$$

So

$$\phi_L = \frac{Fh}{8} r_1 - \frac{F}{2} r_2 \tag{46}$$

We are made

$$\phi_L + \phi_U = \frac{Fh}{4} r_1 \tag{47}$$

Which gives

Penerbit Akademia Baru
Journal of Advanced Research in Fluid Mechanics and Thermal Sciences
ISSN (online): 2289-7879 | Vol. 17, No. 1. Pages 1-17, 2016

$$r_1 = \frac{4(\phi_L + \phi_U)}{Fh} \tag{48}$$

with

$$\phi_L - \phi_U = Fr_2 \tag{49}$$

Which also gives

$$r_2 = \frac{\phi_L + \phi_U}{F} \tag{50}$$

Which gives us the equation (27). The above formulas show once the electrical potential on the upper and lower surfaces of the console which has been obtained from the tests, the piezoelectric parameter (g_{31}) can be identified.

3.5 Identification of the Pyroelectric Coefficient (q_3)

For the case where the console is charged simultaneously by a high temperature and a concentrated force, see Figure 4, the electric potential of the console can be deduced from equation (28) as follows

$$\phi = (\frac{B}{2}z^2 + Az)q_3 - (r_1 z^2 + 2r_2 z)c \tag{51}$$

Moreover, if the symbol (ϕ_{LFT}) is used to record the electrical potential on the upper surface of the beam under thermal and mechanical loads coupled, the pyroelectric coefficient (q_3) can be identified

$$q_3 = \frac{8\phi_{LFT} + (2r_1 h^2 + 8r_2 h)c}{h^2 B + 4hA} = \frac{8\phi_{LFT} + (2r_1 h^2 + 8r_2 h)c}{h\theta_0} \tag{52}$$

For the equation (32), we take the equation (31) and z is replaced by $h/2$ and $\phi = \phi_{LFT}$, The solution of (31) from (q_3) give us the equation (32). If the console is loaded by a thermal loading only, so we

$$q_3 = \frac{8\phi_{LT}}{h\theta_0} \tag{53}$$

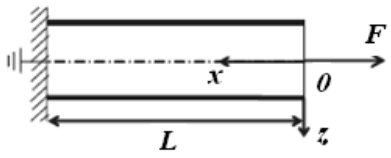

Figure 4: console subject has a concentrated load

Penerbit Akademia Baru

Journal of Advanced Research in Fluid Mechanics and Thermal Sciences
ISSN (online): 2289-7879 | Vol. 17, No. 1. Pages 1-17, 2016

Where the symbol (ϕ_{LT}) denotes the electric potential detected on the lower surface of the console in this case of loading. Equation (38) proves that once the electric potential on the lower surface is detected when the temperature is provided only on the upper surface of the console, in this case the pyroelectric coefficient (q_3) can be identified.

3.6 Special Case Loading and Comparisons

In addition to identifying the hardware settings, the results above is used which can also be used in some special cases of loading leading to simple results. In this part, the two special cases loading are studied. The geometric parameters of the console are covered in this research by [17] are selected, ie, d., $L=16\,mm$ and $h=1.32\,mm$.. Some changes in the physical quantities of the thermal loading on the console are obtained. In addition, the results obtained in this work are compared with those obtained in theoretical and experimental research [18].

3.7 Console only subjected to Thermal Loading

If the console is only subjected to an elevated temperature, the solutions could be directly deduced from the results obtained for the case I assuming that $V_0=0$ and $\xi_{33}\to\infty$ or in the case II assuming $F=0$. In detail, we can obtain the following simple expressions components of the constraint and induction

$$\sigma_x=\sigma_z=\tau_{xz}=D_x=D_z=0 \tag{54}$$

Components of the strain and electric field

$$\begin{cases}\varepsilon_x=-\mu_{11}(A+Bz)\\ \varepsilon_z=-\mu_{33}(A+Bz)\\ \gamma_{xz}=0\\ E_z=-q_3(A+Bz)\\ E_x=0\end{cases} \tag{55}$$

Displacement components and electric potential

$$\begin{cases}u=\mu_{11}(\dfrac{1}{2}-\dfrac{z}{h})(L-x)\theta_0\\ w=-\dfrac{\mu_{33}}{2}(z+\dfrac{z^2}{h})\theta_0+-\dfrac{\mu_{33}}{2h}(x^2-2xL+L^2)\theta_0\\ \phi=\dfrac{q_3}{2}(z+\dfrac{z^2}{h})\theta_0\end{cases} \tag{56}$$

For cadmium selenide console and polarized in the thickness direction, the following hardware settings, $\mu_{11}=-2.16\times10^{-6}\,1/K$, $\mu_{33}=-1.76\times10^{-6}\,1/K$ and $q_3-2.95\times10^4\,N/(KC)$ are used in this study [19]. The longitudinal and transverse displacements of each point on the upper surface of actuator is shown in Figures (5) and (6), respectively, for different temperatures 1, 2 and 5 *K*. FIG (7) shows the distribution of the electric potential at any cross section of the

Penerbit Akademia Baru
Journal of Advanced Research in Fluid Mechanics and Thermal Sciences
ISSN (online): 2289-7879 | Vol. 17, No. 1. Pages 1-17, 2016

beam in different temperatures. This results are consistent with the results obtained by [20]. For a cylindrical axisymmetric violates piezo thermo elastic transversely isotropic finite.

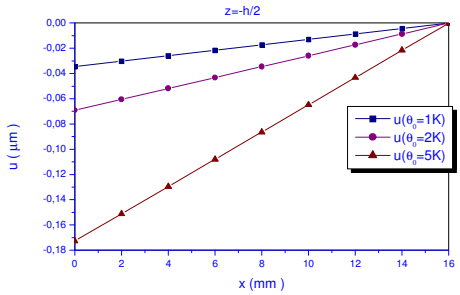

Figure 5: the longitudinal displacement u at $z = -h / 2$

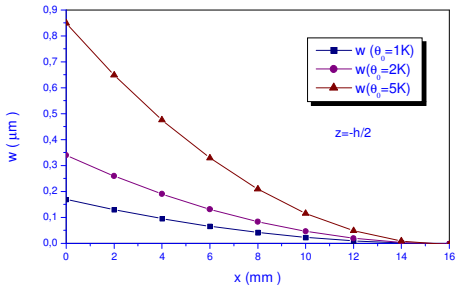

Figure 6: the transverse displacement w a $z = -h / 2$

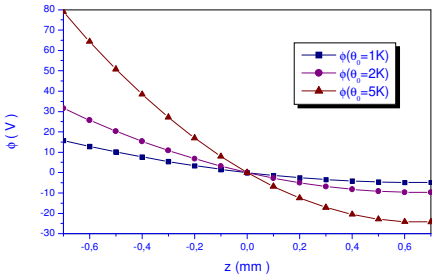

Figure 7: the electric potential distribution has a cross section of console

Console subject only to the electric field:

If the console is only subjected to an electric field, the solutions can be directly deduced from the results obtained if assuming $\theta_0 = 0$ as

Components of the constraint and induction:

$$\sigma_x = \sigma_z = \tau_{xz} = D_x = 0 \qquad D_z = \frac{V_0}{h\xi_{33}} \tag{57}$$

Penerbit Akademia Baru

Journal of Advanced Research in Fluid Mechanics and Thermal Sciences
ISSN (online): 2289-7879 | Vol. 17, No. 1. Pages 1-17, 2016

Components deformation and electric field

$$\begin{cases} \varepsilon_x = \dfrac{V_0}{h\xi_{33}}(r_1 z + r_2)(L - x) \\ \varepsilon_z = \dfrac{V_0 g_{33}}{h\xi_{33}} \\ \gamma_{xz} = 0 \\ E_z = \dfrac{V_0}{h} \\ E_x = 0 \end{cases}$$

Displacement components and electric potential

$$\begin{cases} u = -\dfrac{V_0}{h\xi_{33}}(r_1 z + r_2)(L - x) \\ w = \dfrac{V_0}{h\xi_{33}}[g_{33} z - \dfrac{1}{2} r_1 (x^2 - 2xL + L^2)] \\ \phi = -\dfrac{V_0}{h} z \end{cases} \tag{58}$$

Now we compare the results obtained in this study a few experimental and theoretical results obtained by [20]. Thus, the transverse bending of the console only expressed by an electric voltage charging is rewritten as

$$w = \frac{V_0}{h\xi_{33}}[g_{33} z - \frac{1}{2} r_1 (x^2 - 2xL + L^2)] \tag{59}$$

Based on the theory of elasticity and following the method disclosed by [21] obtained bending (δ) at the free end of the actuator as

$$\delta(N) = \frac{E_3 L^2 d_{31}^{\max}}{h}(\frac{N+1}{N}) \tag{60}$$

$$\mu_{11} = m_1 z + m_2 \qquad \mu_{33} = n_1 z + n_2 \qquad q_3 = t_1 z + t_2 \tag{61}$$

$$\begin{cases} [S_{11}\dfrac{\partial}{\partial z^2} + (S_{13} + \dfrac{S_{44}}{2})\dfrac{\partial^2}{\partial x^2}]\sigma_x + [S_{33}\dfrac{\partial}{\partial x^2} + (S_{13} + \dfrac{S_{44}}{2})\dfrac{\partial^2}{\partial z^2}]\sigma_z + (r_1 z + r_2)\dfrac{\partial^2 D_z}{\partial z^2} \\ + g_{33}\dfrac{\partial^2 D_z}{\partial x^2} + 2r_1\dfrac{\partial D_z}{\partial z} - g_{15}\dfrac{\partial^2 D_x}{\partial x \partial z} - (m_1 z + m_2)\dfrac{\partial^2 \theta}{\partial z^2} - (n_1 z + n_2)\dfrac{\partial^2 \theta}{\partial x^2} = 0 \\ (r_1 z + r_2 + g_{15})\dfrac{\partial \sigma_x}{\partial x} + g_{33}\dfrac{\partial \sigma_z}{\partial x} + \xi_{11}\dfrac{\partial D_x}{\partial z} - \xi_{33}\dfrac{\partial D_z}{\partial x} + (t_1 z + t_2)\dfrac{\partial \theta}{\partial x} = 0 \end{cases} \tag{62}$$

Penerbit Akademia Baru

Journal of Advanced Research in Fluid Mechanics and Thermal Sciences
ISSN (online): 2289-7879 | Vol. 17, No. 1. Pages 1-17, 2016

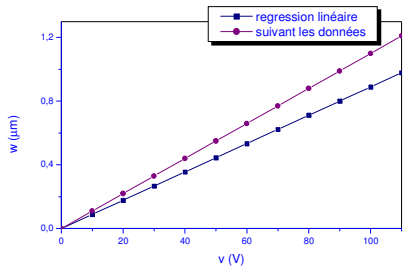

Figure 8: dependence of bending during application of voltage

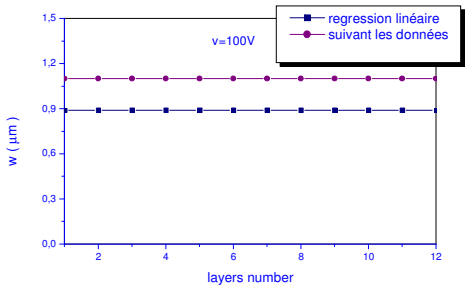

Figure 9: bending actuator rely on a different analytical model *V = 100v*

Where E_3 is the applied electric field, $d_{31}^{\max}$ is the parameter of the lower piezoelectric layer of the beam. In the search [22]. the bending actuators BaTiO3-ceramics, specimens of FGM are composed of N layers with different piezoelectric properties. For simplicity, the dielectric ($\varepsilon_{33}^{T} = 2000F/m$) and other materials parameters are constant for all the layers. In addition, each layer has the same thickness as indicated by the formula $t_L = h/N$ and $h = 1.32mm$ with a surface $16\times4mm^2$. Based on relations piezoelectric parameters, all hardware parameters used in this study including the distribution of the gradient parameter (g_{31}) can be determined for BaTiO3-ceramics. We have, $g_{31} = 45.5zVpm/N$ $(-h/2 \le z \le h/2)$, $g_{33} = 0.08V\ pm/N$ and $\xi_{33} = 0.0005m/F$ According to equation (37), $\delta = w(0,-h/2)$ bending associated with the applied voltage is shown in Figure (8). Celle specifies a slope $m = \frac{\partial w}{\partial V} = 0.0089\mu m/V$. To compare the results, linear regression of experimental data for trimorphic actuator is also shown in the same figure. The regression [22]. Figure 9 shows the relationship between the flexure and the number of the actuator layers (corresponding to an effective field) according to the analytical model and the experimental results of Marcus and according to equation (37) bending determined by this study is to $m = 0.011\mu m/V$, which is also shown in Figure 9. $V = 100\vee$ (fields effective $0.75k\vee/cm$)It can be seen that the bending obtained by experience and by the analytical model N-morph decrease with increasing of number of layers, and the flexure obtained in the present study is slightly smaller than that given by another search based on the model of N-morph. It

is clear that the greater the number of layers increases, the bending back to the result given by equation (51) increases, for actuators FGM.

4.0 DISCUSSION AND CONCLUSION

In the analysis described above, it is assumed that all thermal materials are constant coefficients. The thermal gradient material coefficients with these properties are analyzed. Thermal material parameters (μ_{11}, μ_{33} and q_3) vary linearly along the z direction, which is sufficient for most applications in the technology equations (64),(65), Combining equations (1), (10), and (58), the compatibilizer can be rewritten equation It is clear that the components of the strain and induction as well as the temperature field obtained in this study for each case considered loading satisfy equation (59) .In other words, the linear change thermal material parameters (μ_{11}, μ_{33} and q_3) does not affect the distribution of the stress and the induction for this console. But it has an enormous impact on the stress distribution, the electric field strength, movements and components as well as the electrical potential of the console. Based on the theory of elasticity, the current analysis provides some exact solutions for the piezo-thermoelastic consoles functionally graded in certain cases coupled loads. As inverse problem, the solutions obtained in this present study have been used to determine the gradient profile for the piezoelectric parameter (g_{31}). In the present analysis, the piezoelectric (g_{31}) parameter and the thermal coefficient material (q_3) are identified based on the results of the console under an electric load. It is understandable that the parameters can also be identified in terms of displacement of the console components. The longitudinal displacement changes linearly with the x coordinate in the electrical load and temperature. The plane of the cross section before loading remains the same after loading for the two cases of loading above. The transverse displacement caused by the electric load or the temperature is quadratic with the x coordinate. Electric potential changes linearly with z in the cross-section when the electrical load is applied will be quadratic distribution when the temperature is provided. The bending of the actuator with the gradient behavior is slightly smaller than that of the model N-morph. The more layers of N-morph model increases, the bending decreases result given for FGM actuators.

REFERENCES

[1] P. Bouchilloux, K. Uchino, Combined Finite Element Analysis – Genetic Algorithm Method for the Design of Ultrasonic Motors, Journal of Intelligent Materials Systems and Structures 14 (2003) 657–667.

[2] P. Jane, B. Chris Rhys, Characterization of Mulyi-layer Actuators, Ferroelectrics 273 (2002) 255–260.

[3] Q. Jinhao, T. Junji, U. Toshiyuki, M. Teppei, T. Hirofumi, D. Hejun, Fabrication and High Durability of Functionally Gradient Piezoelectric Bending Actuators, Smart Materials and Structures 12 (2003) 115–121.

[4] S. Raja, K. Rohwer, M. Rose, Piezothermoelastic Modeling and Active Vibration Control of Laminated Composite Beams, Journal of Intelligent Material Systems and Structures 10 (1999) 890–899.

[5] J.N. Reddy, Z. Q. Cheng, Three-Dimensional Solutions of Smart Functionally Graded Plates, Journal of Applied Mechanics 68 (2001) 234-241.

[6] A.J. Ruys, E.B. Popov, D. Sun, J.J. Russell, C.C.J. Murray, Functionally graded electrical/thermal ceramic systems, Journal of the European Ceramic Society21 (2001) 2025-2029.

[7] M.J. Schult, M.J. Sundaresan, M. Jason, D. Clayton, R. Sadler, B. Nagel, Piezoelectric Materials at Elevated Temperature, Journal of Intelligent Materials Systems and Structures 14(2003) 693–705.

[8] Z.F. Shi, General Solution of a Density Functionally Gradient Piezoelectric Cantilever and its Applications, Smart Materials and Structures 11(2002) 122–129.

[9] Z.F. Shi, Y. Chen, Functionally Graded Piezoelectric Cantilever Beam Under Load. Archive of Applied Mechanics 74 (2004) 237–247.

[10] J. Sirohi, I. Chopra, Fundamental Behavior of Piezoceramic Sheet Actuators, Journal of Intelligent Material Systems and Structures 11 (2000) 47–61.

[11] J. Sirohi, I. Chopra, Fundamental Understanding of Piezoelectric Strain Sensors, Journal of Intelligent Material Systems and Structures, 11 (2000) 246–257.

[12] J. Sirohi, I. Chopra, Design and Development of a High Pumping Frequency Piezoelectric-hydraulic Hybrid Actuator, Journal of Intelligent Materials Systems and Structures 14 (2003) 135–147.

[13] I. Tamura, Y. Tomota, M. Ozawa, Strength and ductility of Fe-Ni-C alloys composed of austenite and martensite with various strength, Proceedings of the 3rd International Conference on Strength of Metals and Alloys (1973) 611-615.

[14] X.G. Tian, Y.P. Shen, Finite Element Analysis of Thermo-mechanical Behaviour of Piezoelectric Structures under Finite Deformation, Acta mechanica solida sinica, 24 (2003) 169–178.

[15] C. Va´ zquez, K. Uchino,Novel Piezoelectric-based Power Supply for Driving Piezoelectric Actuators Designed for Active Vibration Damping Applications, Journal of Electroceramics 7 (2001) 197–210.

[16] J. Vendlinski, D. Brei, Dynamic Behavior of Telescopic Actuators, Journal of Intelligent Materials Systems and Structures 14 (2003) 577–586.

[17] B. Victor, Thermal Effects on Measurements of Dynamic Processes in Composite Structures using Piezoelectric Sensors, Smart Materials and Structures 5 (1996) 379–385.

Journal of Advanced Research in Fluid Mechanics and Thermal Sciences
ISSN (online): 2289-7879 | Vol. 17, No. 1. Pages 1-17, 2016

[18] W. Voigt, Über die Beziehung Zwischen den Beiden Elasticitats-Constanten Isotroper Korper, Annalen der Physik and Chemie 38 (1889) 573-587.

[19] F. Weileun, Determination of the Elastic Modulus of Thin Film Materials Using Self-deformed Micromachined Cantilevers, Journal of Micromechanics and Microengineering 9 (1999) 230–235.

[20] Z. Zhong, E.T. Shang, Three Dimensional Exact Analysis of Functionally Gradient Piezothermoelectric Material Rectangular Plate, Acta mechanical sinica 35 (2003) 542–552.

[21] X.H. Zhu, Q. Wang, Z.Y. Meng, A Functionally Gradient Piezoelectric Actuator Prepared by Powder Metallurgical Process in PNN-PZ-PT System, Journal of Materials Science Letters 14 (1995) 516–518.

[22] X. Zhu, J. Xu, Z. Meng, Z. Jianming, S. Zhou, Q. Li, Z. Liu, N. Ming, Microdisplacement characteristics and microstructures of functionally graded piezoelectric ceramic actuator, Materials and Design 21 (2001) 561.